Journal of Cleaner Production 482 (2024) 144209

Contents lists available at ScienceDirect

Journal of Cleaner Production

journal homepage: www.elsevier.com/locate/jclepro

Identification of thresholds and key drivers on water use efficiency in different maize ecoregions in Yellow River Basin of China

Wei Chen [a], Hui Ju [a,b,*], Di Zhang [a,c], William D. Batchelor [d]

[a] Institute of Environment and Sustainable Development in Agriculture, Chinese Academy of Agricultural Sciences, Beijing, 100081, China
[b] Key Laboratory of Agricultural Environment, Ministry of Agriculture and Rural Affaire of PR China, Beijing, 100081, China
[c] Department of Biological Engineering, Yangling Vocational & Technical College, Xianyang, 712000, China
[d] Biosystems Engineering Department, Auburn University, Auburn, AL, 36849, USA

ARTICLE INFO

Handling Editor: Yee Van Fan

Keywords:
Spring maize
Climate change
CERES-Maize model
Drought
Water use efficiency

ABSTRACT

Identifying the constrains on water use efficiency (WUE) of crops along a wet-to-dry gradient is important due to irrigation water scarcity, as well as the increasing drought risk under climate change in China. This study coupled five high-resolution climate models from Coupled Model Intercomparison Project Phase 6 (CMIP6) with the Decision Support System for Agrotechnology Transfer (DSSAT)-CERES-Maize model to quantify drought risk and the drivers affecting WUE in five major maize ecoregions of the Yellow River Basin (YRB) under three future scenarios (SSP126, SSP370, and SSP585) for both the historical baseline (1985–2014) and three future periods: 2021–2040 (2030s), 2041–2070 (2050s), and 2071–2100 (2080s). And a bias correction method was implemented for the crop model to analyze optimal WUE thresholds for maize across varying dry-wet gradients. The results indicated that future drought risk will likely persist in the YRB under all scenarios, but with regional differences in drought severity and frequency. The southwestern region (V) experienced the highest frequency of drought (62.50%-SSP126), while the northwestern region (III) exhibited the lowest frequency (33.00%-SSP585) in 2030s, and 83.30% of areas in the southwestern (V) showed significant wetting in the 2080s under SSP126. The bias-corrected CERES-Maize model effectively simulated crop yield and evapotranspiration (ET), resulting in an average reduction of 4.00% and 9.73% in normalized root mean square error (nRMSE) respectively. Distinct WUE thresholds ranging from 1.96 to 8.41 kg ha^{-1} mm^{-1} were observed across various scenarios-periods in the maize regions, mostly under slight and moderate dry/wet conditions. Notably, all SSP585 scenarios demonstrated a decrease in WUE thresholds compared to the baseline. Across all scenarios and periods, WUE was mainly driven by yield in the eastern regions (I and II) but by ET in the western regions (III, IV, and V). These findings suggest that regions experiencing varying degrees of drought severity should undergo differentiated management and optimization of agricultural practices to improve WUE under future climate scenarios.

1. Introduction

Maize stands as the cornerstone of global food security and plays multiple roles in food, feed, and energy production (Jafari et al., 2024; Li et al., 2023). The YRB is an important maize growing area in China, with 4.86 million hectares of maize plantation, accounting for about 37% of the total arable land in the basin (Liu et al., 2022). As the risks of water pollution and flooding increase (Lan et al., 2024), coupled with the amplifying effects of global warming and the escalating frequency and severity of droughts, maize has emerged as a hotspot for climate disruptions (Rezaei et al., 2023). In particular, drought disturbances severely affect the delicate balance between grain yield and water consumption, resulting in large fluctuations in crop yields (Wang et al., 2020a) and exacerbating the ongoing water crisis (Li et al., 2023).

Drought in many terrestrial regions often arises from reduced precipitation and/or increased evaporation (Dai, 2013), and such droughts tend to be long-lasting and widespread. The dynamics of drought caused by climate change have been extensively studied in maize cultivation areas. For instance, extreme drought events occurring in the U.S. Corn Belt from 1981 to 2016 have been recognized as the primary factor contributing to losses in U.S. maize production (Li et al., 2019). During the same period (1981–2017), the northeastern maize planting areas of China have observed concurrent drought and high temperatures, projected to continue with increasing frequency and intensity from 2021 to 2060 (Li et al., 2022). However, less attention has been paid to the

* Corresponding author. Institute of Environment and Sustainable Development in Agriculture, Chinese Academy of Agricultural Sciences, 100081 Beijing, China.
E-mail address: juhui@caas.cn (H. Ju).

https://doi.org/10.1016/j.jclepro.2024.144209
Received 2 May 2024; Received in revised form 23 October 2024; Accepted 10 November 2024
Available online 12 November 2024

Abbreviations

WUE	Water Use Efficiency
CMIP6	Coupled Model Intercomparison Project Phase 6
DSSAT	Decision Support System for Agrotechnology Transfer
SSP	Shared Socioeconomic Pathway
ET	Evapotranspiration
GCMs	Global Climate Models
SPEI	Standardized Precipitation and Evapotranspiration Index
PET	Potential Evapotranspiration

spatiotemporal variations in drought frequency and trends across maize subdivided ecoregions at different periods under future scenarios, despite the variability of drought occurrences attributable to regional characteristics and temporal changes (Gao et al., 2023; Tripathy et al., 2023). The lack of quantitative studies on drought risks in different maize ecoregions over multiple scenarios-periods leaves a critical information gap, potentially hindering the ability to understand and assess the impacts of drought changes on crops and complicate future context-specific drought risk management.

The core of understanding these risks lies in the challenge of accurately simulating yield-water consumption dynamics, especially in the face of variable and sudden weather events such as drought. Most DSSAT model simulations focus on crop yield (Eitzinger et al., 2017; Cammarano et al., 2022) and quality (Zhang et al., 2023a), yet their performance in capturing the impacts of extreme weather events at the regional level has been suboptimal (Hoogenboom et al., 2019). Current crop models typically underestimate the adverse effects of drought and high-temperature stress on crop yield. Among them, the DSSAT model exhibits the highest explained variance (30%) for maize yield anomalies, surpassing the average of all models (26%) (Heinicke et al., 2022). Furthermore, the CMIP6 meteorological data utilized in the DSSAT model overestimates precipitation (Chai et al., 2022), leading to an overestimation of simulated crop yield to some extent. The model shows acceptable accuracy in simulating ET values under non-water stress conditions (nRMSE = 26.7%); however, it performs poorly under water stress conditions (nRMSE = 43.8%) (Ran et al., 2020). Currently, addressing the simulation deficiencies related to drought effects based on the internal mechanisms of the DSSAT model remains largely unknown (Zhang et al., 2023b). Integrating observational data with crop growth models, along with localized adjustments to internal simulation system parameters and followed by statistical bias correction of the simulated values holds promise for improving the simulation of crop yield and ET.

Water Use Efficiency, defined as the grain yield produced per unit of water used by crops (Tolk et al., 1999) and serves as a crucial parameter for agricultural assessment and water resource management planning (Yu et al., 2020; Wang et al., 2020b). It can be estimated as the ratio of grain yield to seasonal ET at the production level, calculated using simulations from the DSSAT model (Ran et al., 2020; Han et al., 2021). WUE not only influences the linkage between grain yield and water consumption within cropping areas but is also subject to the constraints imposed by drought and environmental factors (Yu et al., 2020). Currently, there is limited information on how WUE of major crops changes under drought conditions, particularly in the compound background of intensifying drought due to global climate change (Mbava et al., 2020). Exploring the patterns and influencing factors of crop WUE under varying wet and dry conditions is essential for understanding and predicting regional grain yield and water consumption coupling responses and feedbacks. However, the strong coupling between the grain yield and water consumption means that changes in WUE simultaneously affect its components (yield or ET) (Jin et al., 2018). Consequently, the importance of comprehensively examining the processes that influence WUE is emphasized for a deeper understanding of grain yield-water consumption process and their response mechanisms to climatic variations.

The objectives of this paper are to: 1) quantify the spatiotemporal changes in drought risk and trends within the spring maize ecoregions of the YRB across historical (1985–2014) and future (2030s, 2050s, 2080s) periods under multiple climate model scenarios; 2) develop a method to reduce biases within the DSSAT model for obtaining more reliable estimates of yield and ET; and 3) investigate the response patterns of WUE under various moisture conditions and the driving mechanisms behind changes in WUE attributed to yield and ET. The results of this study provide a reliable reference for optimizing crop model simulations in other (semi-) arid regions globally and for understanding WUE responses to changes in moisture, with practical guidance offered for managing yield and ET to address the challenges posed by drought under future climate scenarios.

2. Materials and methods

2.1. Study area

The YRB is located in northern China (32°–42°N, 95° to 120°E), spans 795,000 square kilometers, equivalent to 8% of China's total landmass. With a cultivated land area of 13 million hectares (Gao et al., 2023), it boasts a rich variety of crops and serves as a crucial water source, grain-producing region, and ecoregion in China. Maize stands out as the largest cultivated grain crop among the diverse range of crops grown in this basin. Based on the regional classification system for maize cultivation areas in China (Jia et al., 2012), the YRB consists of five major ecoregions dedicated to maize production (Fig. 1).

2.2. DSSAT description and data preparation

The DSSAT model is one of the most widely used crop system models globally, which is commonly used for predicting and assessing grain yield, agricultural management practices, and the impacts of climate change on agriculture (Long et al., 2022; Hoogenboom et al., 2019). The CERES-Maize model (v4.8) is a component of the DSSAT system, capable of simulating key growth and development processes (Si et al., 2021). It was employed to simulate the maize yield, water consumption, and critical phenological stages across five major ecoregions in the YRB. The primary data inputs included crop management practices, daily weather data, soil profile information, and genotype coefficients.

The observational data covering for the period of 1961–2014 at a grid resolution of 0.5° × 0.5° was downloaded from the National Meteorological Information Center of China (http://data.cma.cn/). Daily climate variables included maximum and minimum temperature, precipitation, and sunshine duration (Liu et al., 2014). For this study, the baseline period for climate change assessment was set from 1985 to 2014 (Cui et al., 2023; Liu et al., 2023).

CMIP6 offers various models and simulation data (https://esgf-node.ipsl.upmc.fr/search/cmip6-ipsl/), enabling comprehensive understanding of earth system processes (Wakatsuki et al., 2023; Chai et al., 2022; O'Neill et al., 2016). In this study, daily weather data from five leading global climate models (GCMs) involved in CMIP6 were utilized, covering both historical data and future Shared Socioeconomic Pathways (SSPs). Here, SSP126 is a low-emission scenario, indicating less societal vulnerability and mitigation challenges. SSP370 (medium to high emissions and warming) has been incorporated into IPCC AR6 as a new scenario that can provide more realistic outcomes for climate impacts (Hausfather and Peters, 2020). SSP585 is a scenario with very high emissions. Meanwhile, three time periods were considered: 2030s (near-term), 2050s (mid-term), and 2080s (long-term) to capture the variability of future climate conditions. Considering the variations in original resolutions among GCMs (Table S1), Spatial Disaggregation

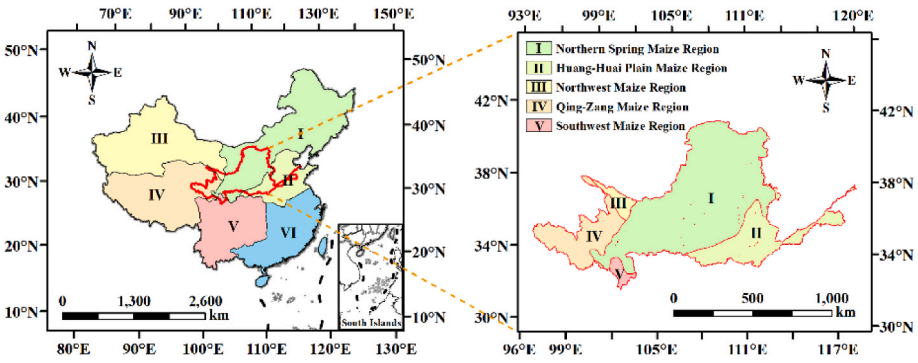

Fig. 1. Five maize ecoregions in the YRB of China.

methods were applied for statistical downscaling and Equidistant Cumulative Distribution Functions were used for bias correction to downscale the climate model data to a 0.5° × 0.5° resolution (Su et al., 2021; Zhang et al., 2023a).

Soil data for each maize planting zone got from the global high-resolution soil profile dataset available at https://dataverse.harvard.edu/. This dataset includes comprehensive soil characteristics like depth, water holding capacity, organic matter content, total nitrogen, pH value, and cation exchange capacity. It was developed using ISRIC's SoilGrids to directly compatible with the DSSAT model soil inputs (Han et al., 2015).

2.3. SPEI index

The Standardized Precipitation and Evapotranspiration Index (SPEI) is a comprehensive index that takes into account both precipitation and Potential Evapotranspiration (PET), enabling accurate calculation and measurement of drought severity (Su et al., 2021; Mishra and Singh, 2010). This study focuses on the growing season (April to October) in the five major spring maize regions of the YRB, so drought conditions were exclusively investigated during this period. The detailed calculation method can be described in Method S1, and the dry-wet classification (9 levels) is shown in Table S2.

2.4. DSSAT-CERES-maize model calibration and evaluation

In this study, the performance of the CERES-Maize model was assessed by simulating key growth stages including flowering and maturity, along with maize yield. The crop production data (n = 54), including growth stages and yield, were collected from agricultural weather stations by the National Meteorological Information Center for model calibration and validation (2001–2006). Meanwhile, the Parameter ESTimation (PEST) method proposed by Ma et al. (2020) in conjunction with trial-and-error calibration was employed to adjust maize genotype coefficients. Region III lacked historical management and yield data records due to the relatively smaller area and coverage primarily consisting of autonomous counties. Given the adjacency of region III to IV, with similar soil conditions and crop varieties, homogeneity in crop growth between regions III and IV was hypothesized based on a representative site located in the intersection of the two regions.

The calibration and validation results were quantified using several statistical indicators, including root mean square error (RMSE), normalized root mean square error (nRMSE), and mean error (ME) (Zhang et al., 2023a; Jiang et al., 2016). The specific calculation formulas are provided in Equations (1)–(3):

$$RMSE = \sqrt{\frac{\sum_{i=1}^{n}(S_i - O_i)}{n}} \quad (1)$$

$$nRMSE = \frac{RMSE}{\overline{O}} \times 100\% \quad (2)$$

$$ME = \frac{1}{n}\sum_{i=1}^{n}(S_i - O_i) \quad (3)$$

Where S_i and O_i represent the simulated and observed values, respectively, while $\overline{O}$ denotes the mean of the observed values, and n stands for the sample size.

Following the calibration and validation of the genetic coefficients, historical and future climate data were used as inputs for the CERES-Maize model to simulate regional maize yield and ET. The crop model simulation was extended from individual field sites to regional scale using the "DSSAT model + Geographic Information System" approach (Lv et al., 2013). The detailed steps for simulating regional yield and ET stated in Method S2.

Additionally, a more reasonable and accurate simulation result correction method was proposed based on the concept of yield gap to mitigate the inherent average bias in regional simulation systems, thereby obtaining more robust estimates of yield/ET. Disparities before and after correction was proposed by selecting a representative grid point at the center of each region for simulation value correction (Eqs. (4)–(6)).

$$SD_{i,j,k} = DSSAT^{Obs}_{i,j,k} - \frac{1}{M}\sum_{m=1}^{M} DSSAT^{Mod_m}_{i,j,k} \quad (4)$$

$$MSB_{j,k} = \frac{1}{N}\sum_{i=1}^{N} SD_{i,j,k} \quad (5)$$

$$CSV_{i,j,k} = MSB_{j,k} + \frac{1}{M}\sum_{m=1}^{M} DSSAT^{Mod_m}_{i,j,k} \quad (6)$$

where SD represents the simulated value difference in year i for grid point (j, k). MSB denotes the mean bias over the years. M denotes the total number of CMIP6 models used, and j,k represent the latitude and longitude of the grid points, respectively. $DSSAT^{Obs}_{i,j,k}$ indicates the DSSAT result as driven by the observed weather data for the baseline period. $DSSAT^{Mod_m}_{i,j,k}$ represents the DSSAT result as driven by the historical simulation from the m-th CMIP6 climate model. N denotes the number of simulation years. The finally corrected simulated value (CSV) equals to the sum of MSB and the average of the $DSSAT^{Mod_m}_{i,j,k}$ results driven by five CMIP6 models' climate simulations.

2.5. Statistical analysis

The Sen's slope estimator is a non-parametric statistic method commonly employed for trend analysis, while the Mann-Kendall (M-K) test is widely utilized to determine the significance of the trend (Wei et al., 2023; Yang et al., 2021). In this study, an integration of Sen's

method with the M-K test was adopted to examine the trends in temperature, precipitation, and SPEI within the maize-growing regions of the YRB. The "trend" package (https://cran.r-project.org/web/packages/trend/index.html) in R was used for this analysis.

This study utilized drought frequency (Fd) as an indicator to assess the variability of drought characteristics in maize regions across the YRB (Omer et al., 2021). Fd was calculated using the formula provided in Equation (7).

$$F_d = d/D \times 100\% \quad (7)$$

where d denotes the count of drought occurrences within the data sequence; D signifies the total number of data sequences.

The trend of SPEI at each grid point was spatially interpolated using the inverse distance weighting method, which performs well when the known points are evenly distributed (Yao et al., 2020).

In this study, WUE (kg ha^{-1} mm^{-1}) was calculated using Equation (8).

$$WUE_{sim\ j,k,i} = Yield_{sim\ j,k,i} \Big/ ET_{sim\ j,k,i} \quad (8)$$

where $Yield_{sim_{j,k,i}}$ is the simulated crop yield (kg ha^{-1}) for grid point (j,k) in year I and $ET_{sim_{j,k,i}}$ is the simulated evapotranspiration (mm) for grid point (j,k) in year i of the maize growth period.

To quantify the driving effects and relative importance of yield and/or ET on changes in WUE, the "ppcor" (https://cran.r-project.org/web/packages/ppcor/index.html) and "relaimpo" (https://cran.r-project.org/web/packages/relaimpo/index.html) packages in R was utilized. The partial correlation focuses primarily on the direct relationship between two variables after controlling for the influence of other variables (Li et al., 2020), while the latter ("relaimpo") is utilized to evaluate the importance of each variable in relation to its overall impact (Zhao et al., 2021).

3. Results

3.1. Drought risk under ensemble of multiple global climate models

3.1.1. Interannual variability of temperature and precipitation

The CMIP6 model ensemble exhibited satisfactory performance in simulating the historical climate of the YRB from 1985 to 2014. The RMSE, nRMSE, and ME between the multi-model annual mean temperature and observations were 0.30 °C, 2.39%, and 0.10 °C (Fig. 2a). Similarly, the model successfully captured the historical variations in average spring maize growing season precipitation in the YRB, with RMSE, nRMSE, and ME values of 6.60 mm mth^{-1}, 10.82% and −2.10 mm mth^{-1}, respectively (Fig. 2b).

In total, significant increases ($p < 0.05$) in temperature and precipitation are projected for the YRB over the next 80 years (Fig. 2). Under the SSP126 scenario, temperature is expected to rise by an average of 1.79 °C (11.37%), accompanied by a monthly increase of 5.67 mm (8.85%) of precipitation compared to historical levels. For the SSP370 scenario, temperature is projected to increase by an average of 2.99 °C (17.64%), with a corresponding monthly precipitation increase of 5.96 mm (9.26%). The largest increases are anticipated under the SSP585 scenario, where temperature and precipitation are estimated to rise by an average of 3.68 °C (20.86%) and 7.51 mm mth^{-1} (11.39%) respectively (Table S3 and Table S4).

3.1.2. Spatiotemporal characteristics of drought risk

The drought risk in the YRB was relatively stable during historical periods, whereas future drought risks exhibited distributed fluctuations

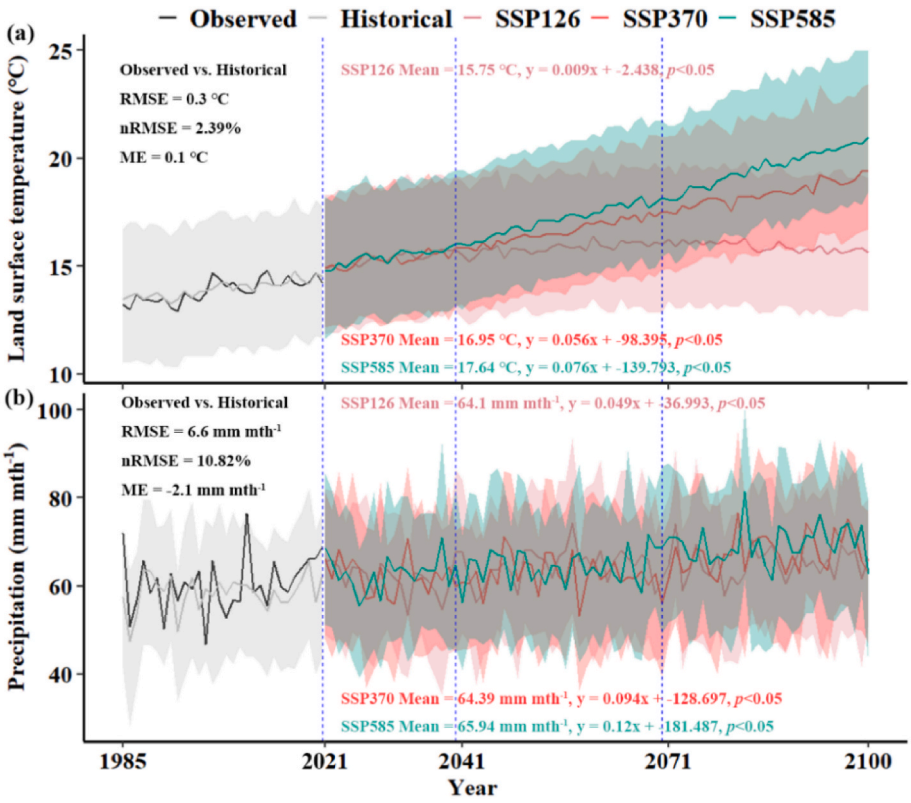

Fig. 2. Land surface air temperature and precipitation in the YRB based on observations and CMIP6 simulations. (a), (b) are the observed (black line) and simulated changes in annual land surface air temperature (°C) and annual mean month precipitation (mm mth^{-1}) during the historical (grey line) period of 1985–2014 and future periods of 2030s, 2050s and 2080s under SSP126 (pink line), SSP370 (red line) and SSP585 (green line) across 5 CMIP6 models. The lines represent the ensemble mean time series, and the shading shows the uncertainty (25%–75%) in terms of the interquartile range across ensemble members.

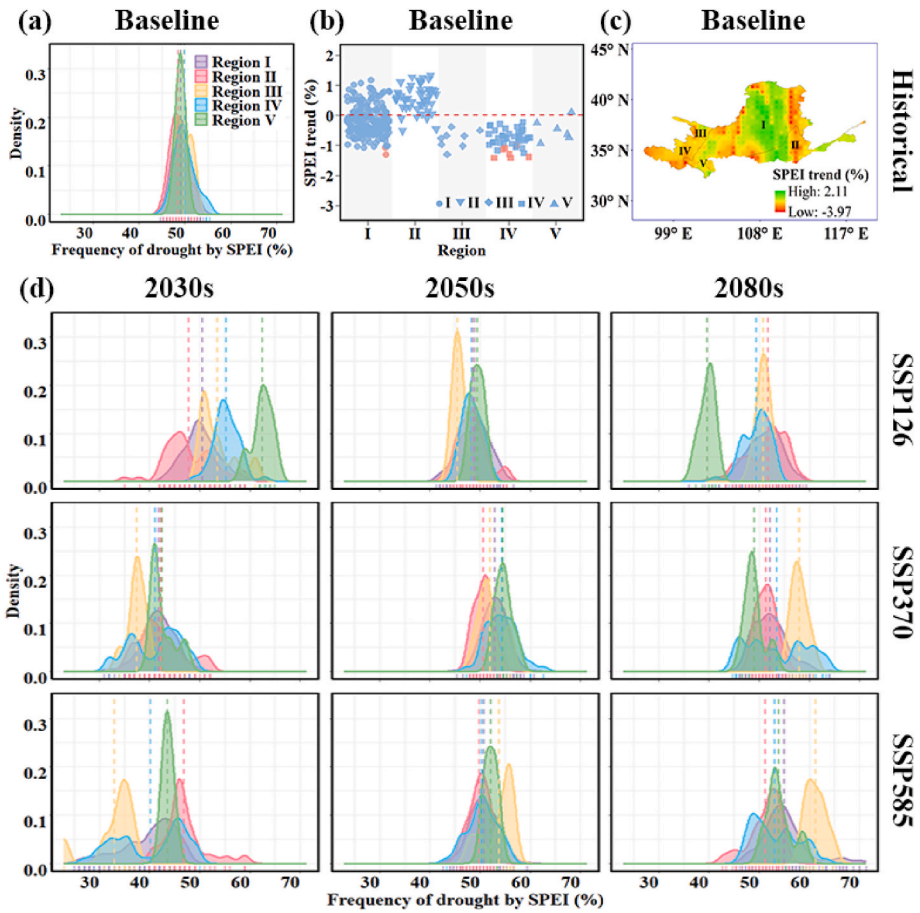

Fig. 3. Drought frequency, SPEI temporal trends and their spatial changes in historical periods, and drought frequency in future periods. (a) The probability density function (PDF) of the drought frequency during the historical (1985–2014) period in each maize ecoregion. The dotted lines of different colors are the mean lines of drought frequency in each maize ecoregion. **(b)** The drought trend of the maize ecoregions in the YRB over the period 1985–2014. The red dotted line in (b) indicates that the SPEI trend is 0. In **(b)**, the rose red symbols represent grid points that had significant trends ($p < 0.05$) in SPEI, while the blue symbols represent grid points with insignificant trends. **(c)** The spatial distribution of SPEI changing trend for the historical period (1985–2014) in the YRB. **(d)** The PDF of the drought frequency during 2021–2040, 2041–2070 and 2071–2100 (columns) and for the SSP126, SSP370 and SSP585 climate scenarios (rows) at the five maize ecoregions in the YRB.

(Fig. 3a–d). Specifically, the average drought frequency ranged between 48.6% and 49.9% during the baseline period in the five major maize-growing regions. Across various future scenarios and periods, 62.2% of the average drought frequencies demonstrated characteristics of increase, while the remaining 37.8% showed a decrease, predominantly occurring in the western regions (III, IV, V) of the YRB. Among these zones, region V under the SSP126 scenario showed the largest increase (13.5%) in drought risk in the 2030s, with an expected frequency as high as 62.5%. Conversely, region III exhibited the lowest future near-term drought risk under the SSP585 scenario (33.0%), indicating a decrease of 16.8%.

The SPEI of most grid points exhibited non-significant trends (Figs. 3b and 4a). Only two grid points in region I and seven grid points in region IV displayed pronounced drought; no statistically significant changes were observed in moisture levels for the remaining 303 grid points (Fig. 3b). There was an overall increase (6.06%) in the number of grid points exhibiting significant changes in moisture conditions across various future scenarios and periods. But this increase only represented 8.94% of all grid points with statistically significant trends in moisture conditions for the future. Region V exhibited a relatively higher proportion (5/6, +83.33%) of significant SPEI trends in the 2080s under SSP126 scenario compared to the other four maize regions (Fig. 4a). Taken together, approximately 91.7% of the dry-wet trends had no significant changes.

The spatial heterogeneity of wet-dry trends across the five maize regions was evident in both historical and future periods (Figs. 3c and 4b). During the baseline period, the SPEI exhibited a pattern of increasing aridity towards the eastern and western ecoregions, while becoming wetter towards the center regions (I and II: the parts of Inner Mongolia, Shaanxi, Gansu, Ningxia), with the declining trend regions covering 66.03% of the total area (Fig. 3c). In the three periods for both the SSP126 and SSP370 scenarios, the eastern portion (I, II) of the YRB experienced increasing aridity throughout the 2030s, with monolithic aridification across the region in the 2050s. However, more than 60% of regions would become wetter in the 2080s compare to the baseline. Conversely, escalating aridity was predicted for the YRB over time under the SSP585 scenario with dry regions continuously expanding beyond the 2030s (Fig. 4b).

3.2. Calibration and validation of DSSAT-CERES-maize model

Comparison between observed and simulated yield, flowering and maturity date from representative sites for the calibration dataset demonstrated that the DSSAT-CERES-Maize model gave accurate simulation results (nRMSE <10%: excellent) for the different regions. The nRMSE between observed and simulated values for yield (HWAM), anthesis date (ADAP), and maturity date (MDAP) were 3.60%–8.51%, 2.30%–9.58%, and 4.19%–8.09%, respectively (Fig. 5 and Table 1).

At the regional level, it was also evident that the overall accuracy of DSSAT-CERES-Maize model simulations is enhanced and deemed acceptable subsequent to correction (Fig. 6). Employing the corrected approach led to an average reduction in errors of 4.00% for yield and

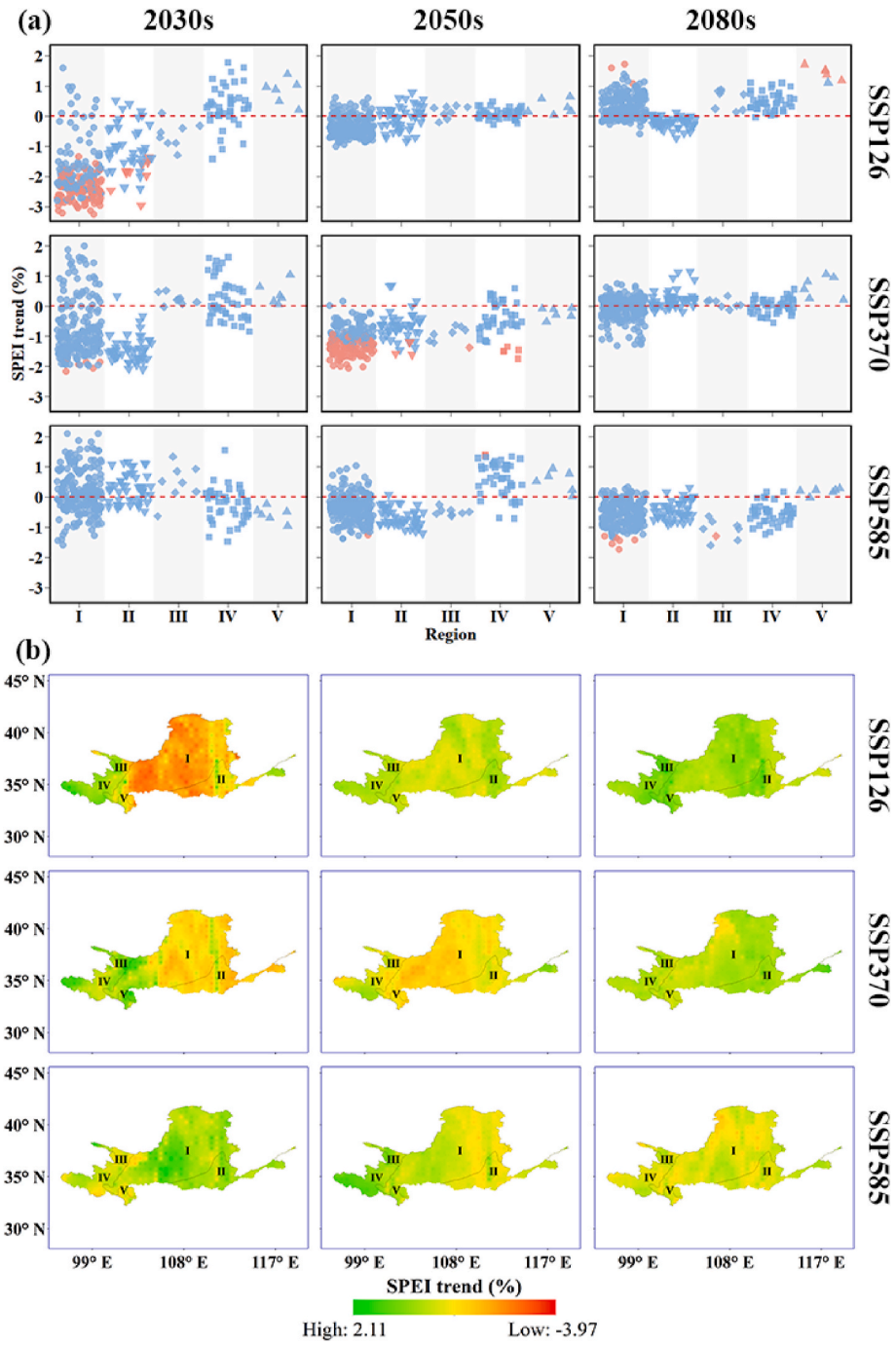

Fig. 4. SPEI temporal trends and their spatial changes in the future. (a) The SPEI trend of the five maize ecoregions (I, II, III, IV, V) in the 2030s, 2050s and 2080s under SSP126, SSP370 and SSP585 scenarios in the YRB. The red dotted line in **(a)** indicates that SPEI trend is 0. In **(a)**, the rose red symbols represent grids that had significant trends ($p < 0.05$) in SPEI, while the blue symbols represent grids with insignificant trends. **(b)** The spatial distribution of SPEI trend in the future periods (2030s, 2050s and 2080s) under three scenarios (SSP126, SSP370, and SSP585) in the subregions of the YRB.

9.73% for ET compared to direct simulation methods. The nRMSE between the simulated values of the representative grid points in each maize region for the historical period and the values estimated from observed grid meteorological data were 13.68%–17.86% (yield) and 10.83%–42.74% (ET), respectively. Following correction based on the concept of yield gap (the average deviation derived from coupled simulation and observation), the nRMSE values for yield and ET ranged from 8.30% to 15.60% and 7.61%–29.24%.

3.3. Response of WUE to drought risk

Few occurrences of severe and extreme conditions were observed across different wet-dry gradient categories in the maize ecoregions (Fig. 7a). The majority of drought and wet events in the maize regions of the YRB were concentrated in the slight to moderate severity levels (42.1%–46.4%) during the reference period, with the proportion of severe and extreme conditions only 0.7%–2.0%. The prevalence of severe and extreme conditions in the future failed to exceed 2.6% compared to the historical period. When aggregating all SPEI categories under future

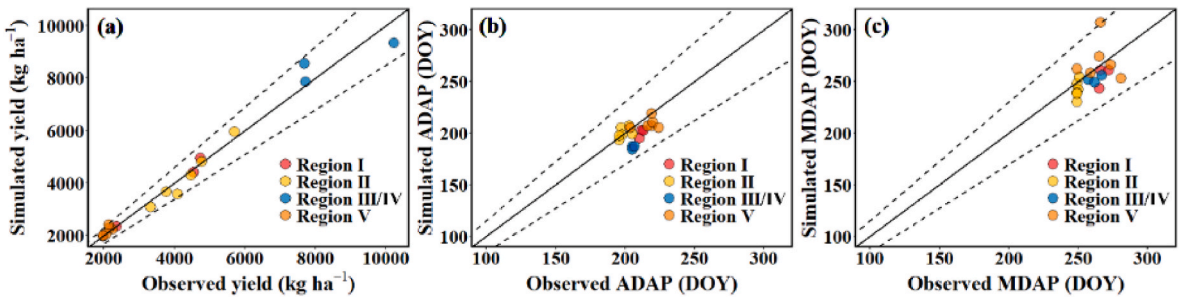

Fig. 5. Comparison between observed and simulated yield at HWAM, ADAP, and MDAP for the representative stations in five regions. The solid black line is the 1:1 reference line and the two black dashed lines represent the upper and lower error bars.

Table 1
Validation of DSSAT-CERES-Maize model for simulating phenology, grain yield for each maize ecoregion in the YRB.

Regional Rep	Region	Year	Parameter	ME (kg ha^{-1})	RMSE (kg ha^{-1})	nRMSE (%)
Xixian	I	2001–2003	Yield	9.67	139.70	3.60
			ADAP	−11.67	11.93	5.64
			MDAP	−12.67	14.49	5.41
Jiexiu	II	2002–2007	Yield	−135.58	273.75	6.29
			ADAP	0.67	4.58	2.30
			MDAP	−7.67	10.46	4.19
Menyuan	III/IV	2001–2003	Yield	32.67	726.98	8.51
			ADAP	−19.67	19.71	9.58
			MDAP	−9.67	10.25	4.38
Pingwu	V	2001–2006	Yield	55.83	114.27	5.45
			ADAP	−8.17	10.70	4.93
			MDAP	4.50	21.47	8.09

Note: III/IV, sharing the same set of crop variety genetic parameters between region III and IV as mentioned in the methods 2.4.

scenario-periods across all regions, only 1.3% were observed to fall within the severe and extreme range.

Next, the response of WUE to varying wet-dry conditions was investigated across multiple scenarios and periods. All maize regions exhibited a peak of WUE under both dry and wet conditions, with WUE predominantly reaching its peak under slight to moderate moisture conditions (Fig. 7b). WUE peak values in regions I-V ranged from 4.2 to 7.3 kg ha^{-1} mm^{-1} during 1985–2014. The future three scenario-periods showed reductions in WUE peaks in comparison with the baseline. Among these, the peak value reduction range (−4.08 ~ −0.74 kg ha^{-1} mm^{-1})in WUE was the most pronounced in the 2080s under SSP585 scenario.

3.4. Contribution of yield and ET on WUE

A consistent strong correlation was observed between yield in region I and II, as well as ET in region IV with WUE across all scenarios and periods, However, the impacts of yield/ET on WUE varied in region III and V (Fig. 8a). Specifically, a significant positive correlation was identified between yield and WUE in region I and II (Pcor: 0.927–0.997, $p < 0.001$), while ET showed a significant negative correlation with WUE in region IV (Pcor: 0.911 ~ −0.953, $p < 0.001$). In partial correlation analysis, irrespective of controlling for yield or ET, the correlation between these two variables and WUE remained highly significant ($p < 0.001$), indicating that yield and ET were pivotal factors impacting WUE variations across scenarios and periods in the five major maize regions (Table S5).

The relative importance of yield and ET in influencing WUE was further analyzed across different maize regions. The findings indicated that WUE in region I and II was predominantly driven by yield, while WUE in region IV and V was mainly influenced by ET. The relative importance of yield (I: 81%–92%, II: 77%–90%) greatly surpassed that of ET in region I and II, while in region IV and V, the relative importance of ET (IV: 64%–70%, V: 52%–64%) slightly outweighed that of yield. However, the dominant factor governing WUE in region III varied across different scenario-periods (Fig. 8b).

4. Discussion

4.1. Drought risk continued with limited exacerbation in the future

The findings indicated that the frequency and intensity of future droughts remain relatively stable, with no clear worsening trend. This finding was consistent with the simulations reported by Leng et al. (2015), which noted that the incidence of meteorological droughts in the YRB from 2020 to 2049 either decreased or remained unchanged under the RCP8.5 scenario compared with 1971–2000. A recent study by Deng et al. (2023) also demonstrated that future drought risk in the upper, middle and lower reaches of the YRB is projected to vary from −1.24 to 0.82 under the SSP585 scenario compared to the baseline period. Nevertheless, attention is still required for drought risk prevention in the YRB. Reducing vulnerability generally takes precedence over overcoming shortfalls when addressing drought risk. The appropriate promotion of fertilization, supplemented by improvements in planting structure, may alleviate this situation.

The results also indicated that the SPEI of most grid points in the five maize regions revealed insignificant trends and exhibited spatial differentiation across various scenarios and time periods. Consistent with previous research on drought in the YRB, SPEI showed a non-significant declining trend during 1985–2014 and 2041–2070 under the SSP585 scenario (Deng et al., 2023). In contrast, an analysis based on data from 124 meteorological stations in the YRB from 1961 to 2015 revealed a non-significant increasing trend in SPEI (Wang et al., 2019). Regarding discrepancies between model predictions and observations, high accuracy was demonstrated between observed and simulated meteorological factors (temperature and precipitation) (Fig. 2). This ensures that the

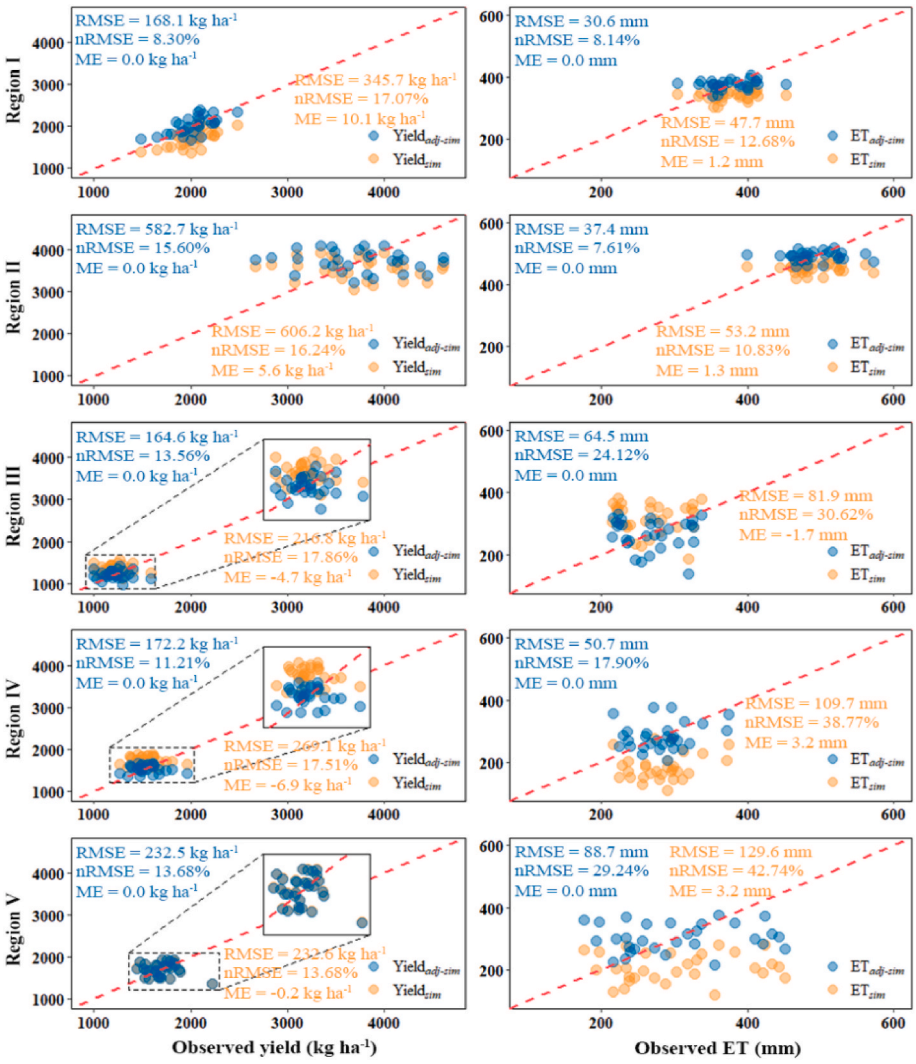

Fig. 6. Comparisons and validations the model simulation values from five CMIP6 models and yield, ET estimates from the coupling observation-simulation correction based on the concept of yield gap against yield and ET measurement results of the 1985–2014 growing season at representative points in the five maize ecoregions in the YRB. Blue and orange solid circles represent data points after and before correction of the model simulation, respectively. The red dashed lines are 1:1 line and the boxes show the effect of the dense scatter points being enlarged.

assessment of trend significance is reliable. This information enhances the applicability and reliability of the results of this study. It further illustrates that although maize-producing areas are susceptible to drought in different scenarios and periods, the overall severity of drought has not increased. The nonsignificance of most SPEI trends may also imply that the exacerbation of drought experienced by local maize regions could be mitigated by relevant climatic factors. On the other hand, the differing SPEI trends among regions necessitate that local agricultural practitioners adopt targeted drought-resistant measures, develop water-saving agriculture, and fully utilize natural precipitation and irrigation water to prevent drought disasters from adversely impacting regional food security (Gao et al., 2023).

The occurrence of severe and extreme wet-dry conditions is rare across maize regions in the YRB as depicted in Fig. 7. These findings align with those reported by Omer et al. (2021), which identified that drought events in the YRB during 1981–2010 were predominantly mild to moderate in severity. Precipitation and temperature represent the most direct factors influencing drought intensity, exerting constraints on both the upper and lower limits of drought severity (Gao et al., 2023). Temperature-driven PET also plays an important role in drought evolution, as higher temperatures generally increase atmospheric water demand, leading to elevated PET (Li et al., 2017; Ohmura and Wild, 2002). The scarcity of severe and extreme wet-dry conditions observed in this study may arise from the interplay among precipitation, temperature, and PET (Fig. 2). These results suggest that future maize cultivation in these areas may not experience significant drought disturbances under various scenarios and periods. The study highlights the interconnectivity between wet-dry variations in the YRB and subdivided maize regions. It provides valuable insights into spatiotemporal dynamics and appropriate combinations of division-scenario-period selections for drought studies.

4.2. *Better performance of the crop model following refined bias correction*

The simulation results of the DSSAT-CERES-Maize model in different ecoregions demonstrated high accuracy, but there were also relative discrete cases of individual data points. On the one hand, it may be attributed to the direct influence of crop genetic parameters. The six parameters in the model are not completely independent; altering one can disrupt the entire simulation results. Among these, the phenological cultivar parameter is the most influential model parameter (Venkatesan and Pazhanivelan, 2018). When investigating the effects of changes in input variables and parameters on model behavior, sensitive parameters

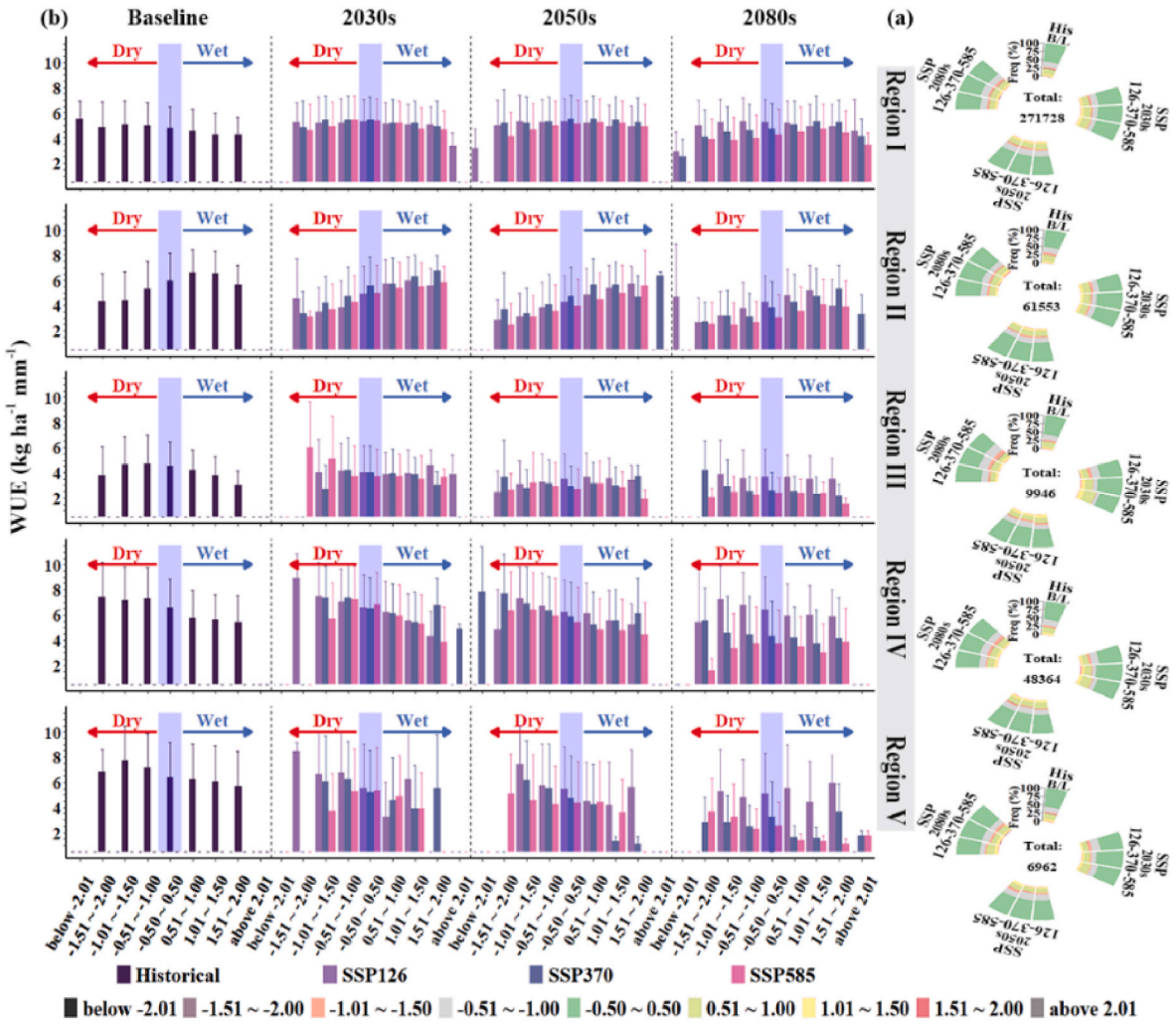

Fig. 7. The relationship between SPEI and WUE. (a) The proportion of various dry and wet moisture gradients in each maize region in the YRB under the four scenarios of Historical, SSP126, SSP370, and SSP585, as well as the four periods of baseline (1985–2014), the future 2030s, 2050s and 2080s. Total represents the number of data points used in the analysis of moisture conditions for each maize region. **(b)** Responses of WUE to drought in the 2030s, 2050s and 2080s under SSP126, SSP370 and SSP585 scenarios for different maize ecoregions. All values are means ± standard deviation (sd). The error bars in all the subplots represent one sd and the shaded area indicates that the moisture status is in the normal category.

should be carefully adjusted. Another possible reason is that errors in ET estimation occur due to the impact of cultivar parameters on water stress sensitivity. Previous studies have shown that there are significant differences in ET between cultivars given the same available water (Thapa et al., 2020). Currently, the cultivar parameters in CERES-Maize do not include sensitivity parameters to water stress, which may lead to suboptimal model performance (Menefee et al., 2021). There are large differences between the simulation results and the data from agricultural meteorological station in certain years, which may also be related to various factors such as observation and sampling.

An effective approach involves obtaining more reliable regional yield/ET estimates by reducing the internal biases of the model system through correction. The current information reflected from relevant studies essentially confirms that the DSSAT model fails to adequately incorporate the impacts of pests, diseases, hail, and freezing on crop yield (Araya et al., 2017). Other global gridded crop models including the DSSAT model will underestimate the future yield decline caused by climate warming (Heinicke et al., 2022). In other words, the yield simulated by the model is an over-estimated result. The DSSAT-CERES-Maize model used to simulate maize water consumption in arid areas also overestimates ET because it fails to perceive any water stress (Ran et al., 2020). This illustrates that the DSSAT model's insensitivity in monitoring factors negatively affecting crop response due to systemic mechanisms in regional applications remains a core problem that needs urgent resolution (Zhang et al., 2023a; Eitzinger et al., 2017). It is strongly suggested that alternatives to the model simulation mechanism be considered until the model system is improved and upgraded (Zhang et al., 2023b). By combining observed weather data with verified CMIP6 data and utilizing a new model correction scheme derived from the concept of yield difference, the average deviation between observation and simulation can be locally adjusted. This integration can enhance the precision of yield and water consumption simulations for the study area. It is noteworthy that no single model (or set of models) outperforms all others across different crops and event types (Heinicke et al., 2022). Therefore, the correction scheme can also serve as a framework for similar studies of other crop models, facilitating precise monitoring of crop yield and water resource security by future crop growth models.

4.3. *WUE thresholds attributed to the linkage of yield and ET*

It was found that the WUE in different maize regions exhibits peaks under both dry and wet conditions; however, the extent of peak WUE varied, indicating the presence of a "threshold" for the impact of

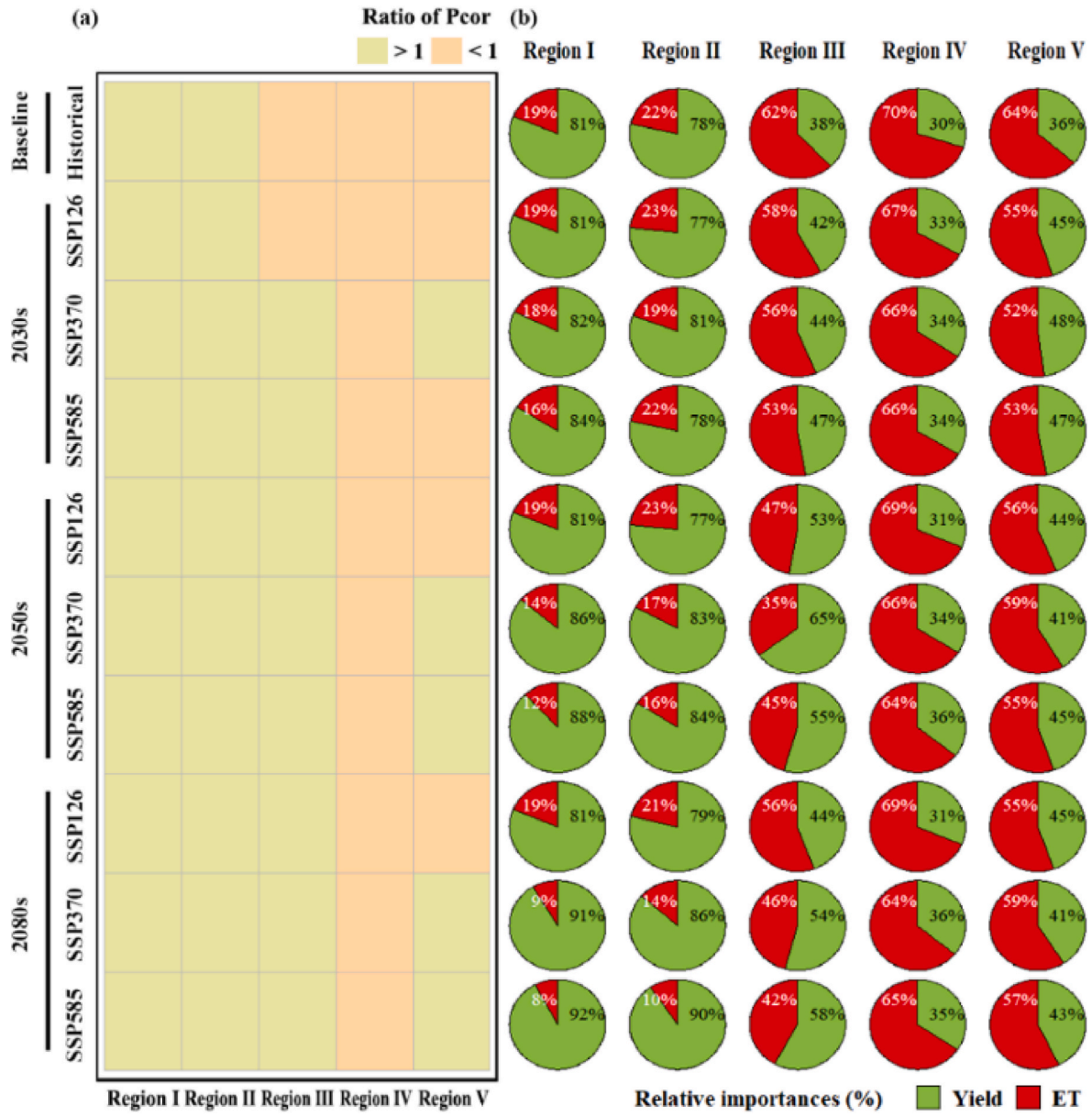

Fig. 8. The dominance of yield and ET over WUE. (a) The ratio of the partial correlation coefficient between WUE and yield to that between WUE and ET in the baseline (1985–2014) and future (2030s, 2050s, 2080s) periods for Historical, SSP126, SSP370 and SSP585 across five CMIP6 models. The light green square indicates that yield plays the dominant role, and the orange pink square indicates that ET plays the dominant role. **(b)** The relative importance (%) of yield (green) and ET (red) variables in influencing WUE across five subregions.

moisture conditions and drought severity on WUE. As previously documented, crop WUE becomes constrained when moisture conditions fall below or exceed this threshold (Zhang et al., 2024; Xu et al., 2019). This phenomenon can be attributed to multiple factors. Soil moisture can both meet the growth needs of crops and avoid adverse effects such as root hypoxia caused by excessive moisture under slight to moderate dry/wet conditions (Fig. 7b). Previous studies have shown that roots penetrate deeper into the soil, enabling more effective water utilization and enhancing crop yield, thereby increasing WUE within a certain range under warm and wet climates (Mbava et al., 2020). In this study, the WUE inflection points predominantly occurred near mild to moderate drought levels, which precisely reflects the physiological adaptive capacity of maize in these regions to environmental changes. Furthermore, the response of WUE to drought also depends on the sensitivity of yield and ET to water deficit, with this sensitivity varying across different climatic zones (Cecil et al., 2023; Lin et al., 2015; Li et al., 2023). Maize grown in semi-arid environments responds more quickly to water limitations (Zou et al., 2021), with a greater decrease in ET compared to yield, thereby increasing WUE. In arid regions, maize as a C4 crop has evolved stronger drought resistance through long-term adaptation to dry conditions (Chipanshi et al., 2003). Conversely, maize has poorer drought adaptability in semi-humid regions. In general, WUE fails to reach peak when water supply is abundant and crop yield is highest (Jin et al., 2018). It should be emphasized that differences in sensitivity to water stress between yield and ET in different maize production regions lead to various response of WUE to drought. This is an important reason for investigating how different wet-dry gradients affect WUE changes.

In this study, it was also observed that yield was the primary driver of WUE in region I and II, while ET was the dominant factor in regions IV and V. This is consistent with previous studies suggesting that the differing influences of yield and ET on WUE may be partly attributed to the geographical and climatic differences among major crop-producing areas in the YRB (Liu et al., 2022). Additionally, no consistent dominant

factor was identified within region III, as corroborated by the ratio of the partial correlation coefficients between yield and ET (Fig. 8a). This inconsistency may be due to the small land area and limited data availability in region III, leading to variability in the results. Given the similarity of crop varieties in regions III and IV, results from region III may be categorized similarly to those from region IV. Crop varieties and fertilization practices are expected to have a more significant impact on maize WUE in regions I and II, while water availability and irrigation management are key determinants in regions III, IV, and V.

4.4. Implication, limitation and future scope

This study holds important implications for assessing the WUE of maize in water-scarce regions under varying wet and dry conditions. The newly developed bias correction method shows that the DSSAT-CERES model can predict yield and ET with greater accuracy across different scenarios. The threshold dynamics of WUE contain abundant feedback information regarding crop yield and ET, enabling a precise decision on whether to prioritize yield enhancement or water-saving strategies to ensure the stability of future maize WUE.

However, this study also has some limitations. (1) Although the historical simulations of the climate model are well aligned with observed values, they are still unable to fully capture the delicate details of extreme weather events (Chai et al., 2022), which may lead to biases when predicting the frequency of extreme high temperatures or heavy rainfall in the future. (2) The focus was primarily on the changes in SPEI under climate conditions, excluding scenarios involving anthropogenic interventions (such as irrigation or water replenishment). (3) In the dynamic physiological process of crop growth, changes in WUE may lag behind the occurrence of meteorological drought, resulting in its underestimation/overestimation. However, the analysis is based on the overall relationship between the established yield/ET ratio and SPEI during the maize growing season over an extended time series, rather than instantaneous changes. Even if there is a lag effect between the two, its impact has been partially smoothed within the time scale, thus not affecting the overall conclusions of this paper. (4) As this study concentrates on the biophysical impacts of climate change on agricultural systems rather than on economic analyses, relevant economic assessments would require additional region-specific economic data and market conditions; therefore, techno-economic estimation is not included so far. Future studies could focus on developing more advanced climate models or integrating larger model ensembles, combined with the bias correction method proposed in this study for crop model simulation outcomes, to better simulate extreme events and reduce the uncertainties derived from the model predictions. Secondly, while meteorological drought can capture the impacts of climate change on maize yield and ET, incorporating more agricultural and hydrological drought indicators would help to improve the accuracy of integrated drought assessments, and thus provide a more comprehensive understanding of the adaptive and regulatory capacity of precision fertilization/irrigation management strategies to the negative effects of climate change. Finally, long-term data regarding yield, water consumption, meteorology, and socioeconomic information from different maize varieties and regions could also be collected and matched accordingly by incorporating crop, climate, and agro-economic models to examine the combined effects of climate change on varietal, regional, and socioeconomic differences.

Despite the above limitations, the proposed model bias correction method provides a new perspective on yield and ET estimations and enhances the practical application to WUE. Compared to traditional drought impact analysis, the multi-moisture gradient analysis implemented in this paper has more clearly physical significance and further refines the dry-wet impacts. Accurately estimating of WUE dynamics in climatically diverse maize ecoregions is critical, and these findings are expected to have broader applicability to other large-scale regions.

5. Conclusions

This study employed CMIP6 climate models and the DSSAT-CERES-Maize model to evaluate the response patterns of WUE to drought, yield, and ET within five maize regions in the YRB. The average drought frequency across the maize ecoregions has been estimated to be 49% (historical) $\pm$ 15.13% (future fluctuation) over time. Future drought risk is expected to increase universally (62%) across all scenarios and periods. The northwestern region (III) exhibited the lowest drought risk under the SSP585 scenario, whereas the southwestern region (V) showed the highest drought risk under SSP126 in the 2030s. Analysis spanning the past 30 years and future 80 years revealed that over 90% of drought trends showed no significant changes, with rare occurrences of severe droughts (1.28%). The newly proposed method for refining simulation results significantly reduced DSSAT model biases in yield (nRMSE: 4.00%) and ET (nRMSE: 9.73%), providing a viable approach for model optimization and application. Comparing the response of WUE to drought in each maize ecoregion, it was found that WUE achieved higher values under slight and moderate moisture conditions in most cases. WUE was primarily driven by yield in the eastern (I and II), while WUE was mainly affected by ET in the western (III, IV, and V) regions. In conclusion, this study helps to understand the water use dynamics under different drought intensities and improve the stability and adaptability of maize yield. The relative contribution of yield and ET changes caused by climate factors to WUE may change with increasing future temperatures and drought, which is more convincing when combined with crop ecoregionalization. It also provides guidance for the future research on the coupling relationship between irrigation and fertilization strategies and grain yield-water consumption according to local conditions.

CRediT authorship contribution statement

Wei Chen: Writing – review & editing, Writing – original draft, Visualization, Software, Methodology, Formal analysis. **Hui Ju:** Writing – review & editing, Validation, Supervision, Software, Resources, Project administration, Methodology, Funding acquisition, Data curation, Conceptualization. **Di Zhang:** Software, Data curation. **William D. Batchelor:** Writing – review & editing, Validation, Software.

Declarations

The authors declare that they have no known competing financial interests or personal relationships that could have appeared to influence the work reported in this paper.

Funding

The study was supported by the National Key Research and Development Program of China (2019YFA0607403; 2023YFD1701902), Asia-Pacific Network for Global Change Research (APN CBA2023-02MY-Ju), and Science and Technology Innovation Project of CAAS (2020–2025).

Declaration of competing interest

The authors declare that they have no known competing financial interests or personal relationships that could have appeared to influence the work reported in this paper.

Acknowledgments

We recognize the support of Chinese Academy of Agricultural Sciences, Ministry of Water Resources of the People's Republic of China and Ministry of Agriculture and Rural Affaire of P.R.China.

Appendix A. Supplementary data

Supplementary data to this article can be found online at https://doi.org/10.1016/j.jclepro.2024.144209.

Data availability

Data will be made available on request.

References

Araya, A., Kisekka, I., Gowda, P.H., Prasad, P.V.V., 2017. Evaluation of water-limited cropping systems in a semi-arid climate using DSSAT-CSM. Agric. Syst. 150, 86–98.

Cammarano, D., Jamshidi, S., Hoogenboom, G., Ruane, A.C., Niyogi, D., Ronga, D., 2022. Processing tomato production is expected to decrease by 2050 due to the projected increase in temperature. Nat. Food 3, 437–444.

Cecil, M., Chilenga, A., Chisanga, C., Gatti, N., Krell, N., Vergopolan, N., Baylis, K., Caylor, K., Evans, T., Konar, M., Sheffield, J., Estes, L., 2023. How much control do smallholder maize farmers have over yield? Field Crops Res. 301.

Chai, Y., Yue, Y., Slater, L.J., Yin, J., Borthwick, A.G.L., Chen, T., Wang, G., 2022. Constrained CMIP6 projections indicate less warming and a slower increase in water availability across Asia. Nat. Commun. 13.

Chipanshi, A., Chanda, R., Totolo, O., 2003. Vulnerability assessment of the maize and sorghum crops to climate change in Botswana. Climatic Change 61, 339–360.

Cui, T., Li, Y., Yang, L., Nan, Y., Li, K., Tudaji, M., Hu, H., Long, D., Shahid, M., Mubeen, A., He, Z., Yong, B., Lu, H., Li, C., Ni, G., Hu, C., Tian, F., 2023. Non-monotonic changes in Asian Water Towers' streamflow at increasing warming levels. Nat. Commun. 14.

Dai, A., 2013. Increasing drought under global warming in observations and models. Nat. Clim. Change 3, 52–58.

Deng, H., Yin, Y., Zong, X., Yin, M., 2023. Future drought risks in the Yellow River Basin and suggestions for targeted response. Int. J. Disaster Risk Reduc. 93.

Eitzinger, A., Laderach, P., Rodriguez, B., Fisher, M., Beebe, S., Sonder, K., Schmidt, A., 2017. Assessing high-impact spots of climate change: spatial yield simulations with Decision Support System for Agrotechnology Transfer (DSSAT) model. Mitig. Adapt. Strategies Glob. Change 22, 743–760.

Gao, Y., Fu, S., Cui, H., Cao, Q., Wang, Z., Zhang, Z., Wu, Q., Qiao, J., 2023. Identifying the spatio-temporal pattern of drought characteristics and its constraint factors in the Yellow River Basin. Ecol. Indicat. 154.

Han, E., Ines, A., Koo, J., 2015. Global high-resolution soil profile database for crop modeling applications. Harvard Dataverse 1, 1–37.

Han, Z., Zhang, B., Yang, L., He, C., 2021. Assessment of the impact of future climate change on maize yield and water use efficiency in agro-pastoral ecotone of Northwestern China. J. Agron. Crop Sci. 207, 317–331.

Hausfather, Z., Peters, G.P., 2020. Emissions–the 'business as usual'story is misleading. Nature 577, 618–620.

Heinicke, S., Frieler, K., Jägermeyr, J., Mengel, M., 2022. Global gridded crop models underestimate yield responses to droughts and heatwaves. Environ. Res. Lett. 17.

Hoogenboom, G., Porter, C.H., Boote, K.J., Shelia, V., Wilkens, P.W., Singh, U., White, J. W., Asseng, S., Lizaso, J.I., Moreno, L.P., 2019. The DSSAT Crop Modeling Ecosystem. Advances in Crop Modelling for a Sustainable Agriculture. Burleigh Dodds Science Publishing.

Jafari, F., Wang, B., Wang, H., Zou, J., 2024. Breeding maize of ideal plant architecture for high-density planting tolerance through modulating shade avoidance response and beyond. J. Integr. Plant Biol. 66 (5), 849–864.

Jia, H., Wang, J., Cao, C., Pan, D., Shi, P., 2012. Maize drought disaster risk assessment of China based on EPIC model. Int. J. Digital Earth 5, 488–515.

Jiang, Y., Zhang, L., Zhang, B., He, C., Jin, X., Bai, X., 2016. Modeling irrigation management for water conservation by DSSAT-maize model in arid northwestern China. Agric. Water Manag. 177, 37–45.

Jin, N., Ren, W., Tao, B., He, L., Ren, Q., Li, S., Yu, Q., 2018. Effects of water stress on water use efficiency of irrigated and rainfed wheat in the Loess Plateau, China. Sci. Total Environ. 642, 1–11.

Lan, H., Zhao, Z., Li, L., Li, J., Fu, B., Tian, N., Lai, R., Zhou, S., Zhu, Y., Zhang, F., Peng, J., Clague, J.J., 2024. Climate change drives flooding risk increases in the Yellow River Basin. Geog. Sustain. 5(2), 193-199.

Leng, Guoyong, Tang, Qiuhong, Rayburg, S., 2015. Climate change impacts on meteorological, agricultural and hydrological droughts in China. Global Planet. Change 126, 23–34.

Li, Z., Chen, Y., Fang, G., Li, Y., 2017. Multivariate assessment and attribution of droughts in Central Asia. Sci. Rep. 7, 1316.

Li, Y., Guan, K., Schnitkey, G.D., Delucia, E., Peng, B., 2019. Excessive rainfall leads to maize yield loss of a comparable magnitude to extreme drought in the United States. Global Change Biol. 25, 2325–2337.

Li, Z., Li, Z., Tong, X., Zhang, J., Dong, L., Zheng, Y., Ma, W., Zhao, L., Wang, L., Wen, L., 2020. Climatic humidity mediates the strength of the species richness–biomass relationship on the Mongolian Plateau steppe. Sci. Total Environ. 718, 137252.

Li, E., Zhao, J., Pullens, J.W.M., Yang, X., 2022. The compound effects of drought and high temperature stresses will be the main constraints on maize yield in Northeast China. Sci. Total Environ. 812, 152461.

Li, X., Zhang, Y., Ma, N., Zhang, X., Tian, J., Zhang, L., Mcvicar, T.R., Wang, E., Xu, J., 2023. Increased grain crop production intensifies the water crisis in Northern China. Earth's Future 11, e2023EF003608.

Lin, Y., Wu, W., Ge, Q., 2015. CERES-Maize model-based simulation of climate change impacts on maize yields and potential adaptive measures in Heilongjiang Province, China. J. Sci. Food Agric. 95, 2838–2849.

Liu, X., Li, Y., Zhong, X., Zhao, C., Jensen, J.R., Zhao, Y., 2014. Towards increasing availability of the Ångström–Prescott radiation parameters across China: spatial trend and modeling. Energy Convers. Manag. 87, 975–989.

Liu, Y., Lin, Y., Huo, Z., Zhang, C., Wang, C., Xue, J., Huang, G., 2022. Spatio-temporal variation of irrigation water requirements for wheat and maize in the Yellow River Basin, China, 1974–2017. Agric. Water Manag. 262.

Liu, L., He, G., Wu, M., Liu, G., Zhang, H., Chen, Y., Shen, J., Li, S., 2023. Climate change impacts on planned supply–demand match in global wind and solar energy systems. Nat. Energy 8, 870–880.

Long, X.-X., Ju, H., Wang, J.-D., Gong, S.-H., Li, G.-Y., 2022. Impact of climate change on wheat yield and quality in the Yellow River Basin under RCP8.5 during 2020–2050. Adv. Clim. Change Res. 13, 397–407.

Lv, Z., Liu, X., Cao, W., Zhu, Y., 2013. Climate change impacts on regional winter wheat production in main wheat production regions of China. Agric. For. Meteorol. 171–172, 234–248.

Ma, H., Malone, R.W., Jiang, T., Yao, N., Chen, S., Song, L., Feng, H., Yu, Q., He, J., 2020. Estimating crop genetic parameters for DSSAT with modified PEST software. Eur. J. Agron. 115.

Mbava, N., Mutema, M., Zengeni, R., Shimelis, H., Chaplot, V., 2020. Factors affecting crop water use efficiency: a worldwide meta-analysis. Agric. Water Manag. 228.

Menefee, D., Rajan, N., Cui, S., Bagavathiannan, M., Schnell, R., West, J., 2021. Simulation of dryland maize growth and evapotranspiration using DSSAT-CERES-Maize model. Agron. J. 113, 1317–1332.

Mishra, A.K., Singh, V.P., 2010. A review of drought concepts. J. Hydrol. 391, 202–216.

O'neill, B.C., Tebaldi, C., Van Vuuren, D.P., Eyring, V., Friedlingstein, P., Hurtt, G., Knutti, R., Kriegler, E., Lamarque, J.-F., Lowe, J., Meehl, G.A., Moss, R., Riahi, K., Sanderson, B.M., 2016. The scenario model Intercomparison Project (ScenarioMIP) for CMIP6. Geosci. Model Dev. (GMD) 9, 3461–3482.

Ohmura, A., Wild, M., 2002. Is the hydrological cycle accelerating? Science 298, 1345–1346.

Omer, A., Zhuguo, M., Yuan, X., Zheng, Z., Saleem, F., 2021. A hydrological perspective on drought risk-assessment in the Yellow River Basin under future anthropogenic activities. J. Environ. Manag. 289.

Ran, H., Kang, S., Hu, X., Li, S., Wang, W., Liu, F., 2020. Capability of a solar energy-driven crop model for simulating water consumption and yield of maize and its comparison with a water-driven crop model. Agric. For. Meteorol. 287.

Rezaei, E.E., Webber, H., Asseng, S., Boote, K., Durand, J.L., Ewert, F., Martre, P., Maccarthy, D.S., 2023. Climate change impacts on crop yields. Nat. Rev. Earth Environ. 4, 831–846.

Si, Z., Zain, M., Li, S., Liu, J., Liang, Y., Gao, Y., Duan, A., 2021. Optimizing nitrogen application for drip-irrigated winter wheat using the DSSAT-CERES-Wheat model. Agric. Water Manag. 244.

Su, B., Huang, J., Mondal, S.K., Zhai, J., Wang, Y., Wen, S., Gao, M., Lv, Y., Jiang, S., Jiang, T., Li, A., 2021. Insight from CMIP6 SSP-RCP scenarios for future drought characteristics in China. Atmos. Res. 250.

Thapa, S., Xue, Q., Marek, T.H., Xu, W., Porter, D., Jessup, K.E., 2020. Corn production under restricted irrigation in the Texas High Plains. Agron. J. 112, 1190–1200.

Tolk, J.A., Howell, T.A., R, E.S., 1999. Effect of mulch, irrigation, and soil type on water use and yield of maize. Soil Tillage Res. 50, 137–147.

Tripathy, K.P., Mukherjee, S., Mishra, A.K., Mann, M.E., Williams, A.P., 2023. Climate change will accelerate the high-end risk of compound drought and heatwave events. In: Proceedings of the National Academy of Sciences, vol. 120, e2219825120.

Venkatesan, M., Pazhanivelan, S., 2018. Estimation of maize yield at spatial level using DSSAT crop simulation model. Madras Agric. J.105, 548-552.

Wakatsuki, H., Ju, H., Nelson, G.C., Farrell, A.D., Deryng, D., Meza, F., Hasegawa, T., 2023. Research trends and gaps in climate change impacts and adaptation potentials in major crops. Curr. Opin. Environ. Sustain. 60.

Wang, F., Wang, Z., Yang, H., Zhao, Y., Zhang, Z., Li, Z., Hussain, Z., 2019. Copula-based drought analysis using standardized precipitation evapotranspiration index: a case study in the Yellow River Basin, China. Water 11.

Wang, X., Zhao, C., Müller, C., Wang, C., Ciais, P., Janssens, I., Peñuelas, J., Asseng, S., Li, T., Elliott, J., 2020a. Emergent constraint on crop yield response to warmer temperature from field experiments. Nat. Sustain. 3, 908–916.

Wang, Y., Guo, T., Qi, L., Zeng, H., Liang, Y., Wei, S., Gao, F., Wang, L., Zhang, R., Jia, Z., 2020b. Meta-analysis of ridge-furrow cultivation effects on maize production and water use efficiency. Agric. Water Manag. 234.

Wei, C., Shuguang, L., Shuqing, Z., Yu, Z., Shuailong, F., Zhao, W., Yiping, W., Jingfeng, X., Wenping, Y., Wende, Y., Hui, J., Qinyi, W., 2023. Temporal dynamics of ecosystem, inherent, and underlying water use efficiencies of forests, grasslands, and croplands and their responses to climate change. Carbon Bal. Manag. 18.

Xu, H.-J., Wang, X.-P., Zhao, C.-Y., Zhang, X.-X., 2019. Responses of ecosystem water use efficiency to meteorological drought under different biomes and drought magnitudes in northern China. Agric. For. Meteorol. 278.

Yang, S., Zhang, J., Han, J., Wang, J., Zhang, S., Bai, Y., Cao, D., Xun, L., Zheng, M., Chen, H., Xu, C., Rong, Y., 2021. Evaluating global ecosystem water use efficiency response to drought based on multi-model analysis. Sci. Total Environ. 778, 146356.

Yao, N., Li, L., Feng, P., Feng, H., Li Liu, D., Liu, Y., Jiang, K., Hu, X., Li, Y., 2020. Projections of drought characteristics in China based on a standardized precipitation and evapotranspiration index and multiple GCMs. Sci. Total Environ. 704.

Yu, L., Gao, X., Zhao, X., 2020. Global synthesis of the impact of droughts on crops' water-use efficiency (WUE): towards both high WUE and productivity. Agric. Syst. 177.

Zhang, D., Liu, J., Li, D., Batchelor, W.D., Wu, D., Zhen, X., Ju, H., 2023a. Future climate change impacts on wheat grain yield and protein in the North China Region. Sci. Total Environ. 166147.
Zhang, H., Zhao, T., Ji, R., Chang, S., Gao, Q., Zhang, G., 2023b. The decreased availability of soil moisture and canopy conductance dominate evapotranspiration in a rain-fed maize ecosystem in northeastern China. Agronomy 13.
Zhang, J., Tian, H., Li, X., Qin, X., Fang, S., Zhang, J., Zhang, W., Wang, S., Pan, S., 2024. A warmer and wetter world would aggravate GHG emissions intensity in China's cropland. Earth's Future 12.
Zhao, J., Feng, H., Xu, T., Xiao, J., Guerrieri, R., Liu, S., Wu, X., He, X., He, X., 2021. Physiological and environmental control on ecosystem water use efficiency in response to drought across the northern hemisphere. Sci. Total Environ. 758, 143599.
Zou, Y., Saddique, Q., Ali, A., Xu, J., Khan, M.I., Qing, M., Azmat, M., Cai, H., Siddique, K.H.M., 2021. Deficit irrigation improves maize yield and water use efficiency in a semi-arid environment. Agric. Water Manag. 243.